ISSN PRINT 2319 1775 Online 2320 7876

Research paper UGC CARE Listed (Group -I) Journal Volume 10, Spl Iss 2, 2021

Throughout the 24th solar cycle, we simulate and examine the low latitude climatology of the GPS-TEC using empirical orthogonal functions

D. Venkata Ratnam

Department of ECE, Koneru Lakshmaiah Education Foundation, Green Fields, Vaddeswaram, Andhra Pradesh 522 502, India.

K Sri Charan, Department of ECE, Koneru Lakshmaiah Education Foundation Hyderabad India-500075, sricharan.kaipa@gmail.com

Abstract

The data spans an extended period from 2009 to 2016, covering the 24th solar cycle. The EOF model decomposes the TEC data into base functions and corresponding coefficients, effectively capturing the influence of solar and geomagnetic activity on TEC variations.The first three EOF modes account for approximately 98% of the total variance in the observed data, indicating their significance in representing the temporal and spatial characteristics of the ionosphere. To characterize the solar-cycle, annual, and semi-annual dependencies, the Fourier Series Analysis (FSA) is applied to modulate the first three EOF coefficients with solar (F10.7) and geomagnetic (Ap and Dst) indices. The TEC model is validated under various solar and geomagnetic conditions, including daytime and nighttime periods. The study finds a positive correlation (0.85) between averaged daily GPS-TEC and averaged daily F10.7, indicating the ionosphere's time-varying characteristics dependent on solar activity. The EOF model's validity and reliability are assessed by comparing it with GPS-TEC data and standard global ionospheric models (IRI2016 and SPIM). The performance of the standard ionospheric models is relatively better during High Solar Activity (HSA) periods compared to Low Solar Activity (LSA) periods. The paper showcases the utility of the EOF model in understanding and characterizing ionospheric behavior under different solar and geomagnetic conditions.

Introduction

By introducing range delays in the sent signals, the ionospheric electron density and its spatiotemporal changes play a vital role in applications for trans ionospheric navigation and communication systems [1]. The solar and magnetospheric effects, momentum and energy effects related to neutral wind dynamics, and lithospheric effects all play a role in the variability of the ionospheric electron density. Total Electron Content (TEC) is a crucial parameter for measuring ionospheric electron density and assessing delays experienced by Global

ISSN PRINT 2319 1775 Online 2320 7876

Research paper UGC CARE Listed (Group -I) Journal Volume 10, Spl Iss 2, 2021

Positioning System (GPS) signals as they traverse through the ionosphere. TEC exhibits spatial and temporal variations, with higher magnitudes observed in equatorial and low latitude regions due to latitudinal and longitudinal gradients [2]. Estimating TEC in the equatorial and low latitude region is particularly challenging due to the significant spatio-temporal gradients caused by local electrodynamic factors like Equatorial Electrojet (EEJ) strength and Equatorial Ionization Anomaly (EIA). Accurate determination of TEC in these regions is essential for various applications relying on GPS signals [3].

Previous scholars offered empirical modelling to meet the needs of scientific and technical application based on the GPS-TEC observations. These include the International Reference Ionosphere (IRI) model [4-6], Incoherent Scatter Radar (ISR)-based Ionospheric Model, and Empirical Storm-Time Ionospheric Correction Model (STORM). Based on solar (F10.7) and geomagnetic (Ap) indices as a function of Local Time (LT), latitude, and season, these models estimate various ionospheric parameters, including NmF2, hmF2, foF2, and ion temperatures at any location [7]. Numerous authors have conducted extensive research to construct the global and regional ionospheric TEC models utilising a variety of methodologies, including statistical Eigen Mode (EM) and Principal Component Analysis. Spherical Cap Harmonic Analysis (SCHA), Singular Value Decomposition (SVD) and Empirical Orthogonal Function (EOF) involving Taylor series as well as Fourier series expansion techniques [8-10]. Regional ionospheric Total Electron Content (TEC) models differ from global ionospheric models as they focus on specific geographical regions and incorporate local driving phenomena, providing a clearer ionospheric prediction. Several regional TEC models have been proposed for different territories, including China, Denmark, Japan, Southern Africa, and the Indian sub-continent. Studies analyzing ionospheric TEC variations in the equatorial and low latitude region over the Indian sub-continent have contributed to improving the climatological accuracy of the International Reference Ionosphere (IRI) model to some extent [11-13]. These regional models take into account local factors like the equatorial ionization anomaly (EIA) phenomena and the solar-terrestrial and geomagnetic effects to better characterize the ionospheric morphology in specific areas.

1. modelling and processing of data

Ionospheric parameters from 2009 to 2016 are taken into account over Bangalore, India (13.02° N, 77.57° E). Every 30 seconds, the observations were recorded at ftp://cddis.gsfc.nasa.gov. Using GPSTEC software, RINEX observation data are extracted to Slant TEC (STEC)-measurements [14-15]. To translate STEC results into vertical TEC (VTEC) values, a single

ISSN PRINT 2319 1775 Online 2320 7876

Research paper UGC CARE Listed (Group -I) Journal Volume 10, Spl Iss 2, 2021

layer approximation is used, with the ionospheric Pierce Point (IPP) taken into account at an altitude of 350 km above the surface of the planet.

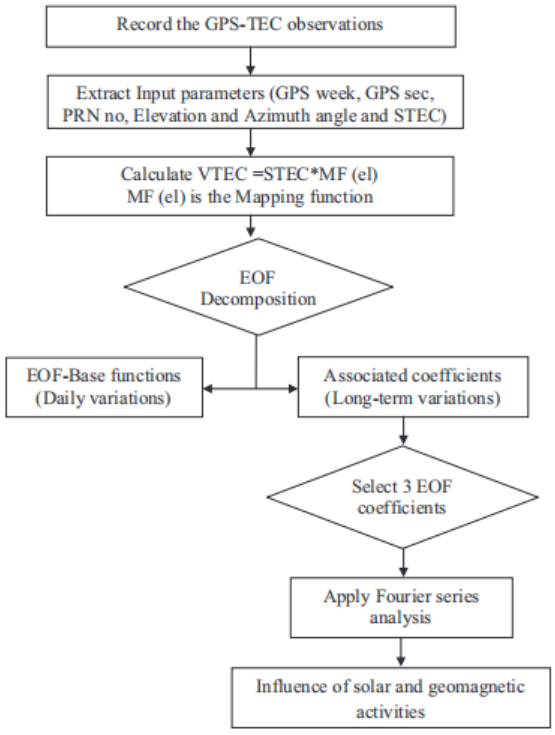

$$Correl.Coeff = \frac{\sum_i (X_i - \overline{X_i}) - (Y_i - \overline{Y_i})}{\sqrt{\sum_i (X_i - \overline{X_i})^2 - \sum_i (Y_i - \overline{Y_i})^2}} \quad (7)$$

$$RMSD = \sqrt{\frac{\sum_{i=1}^{n} (X_i - Y_i)^2}{n}} \quad (8)$$

Percentage of RMSD computed as

$$RMSD\ (\%) = \frac{RMSD}{RMS_{obs}} \times 100 \quad (9)$$

where

$$RMS_{obs} = \sqrt{\frac{\sum_i^n (X_i)^2}{n}}$$

where n is the number of TEC observations, Xi denotes the respective observed TEC data, Xi is their mean, Y i denotes the corresponding model TEC data, Y i is their mean, the subscripts 'i' identify numerical places in the data, and so forth.

2. Results

ISSN PRINT 2319 1775 Online 2320 7876

Research paper UGC CARE Listed (Group -I) Journal Volume 10, Spl Iss 2, 2021

The study focuses on the ionospheric variability and characteristics over the northern low-latitude region of Bangalore during the 24th solar cycle (2009–2016) using GPS-TEC observational data. Figure 2 illustrates the temporal variations of GPS-TEC in the near-equatorial location of Bangalore. The TEC data shows a double-humped structure with secondary maxima appearing in the late evening hours during equinoctial months. This pattern is associated with the pre-reversal enhancement (PRE) effect, which occurs due to the day-night reversal of wind at the terminator. During the Low Solar Activity (LSA) period, diurnal VTEC peak values of around 15–25 TECU are observed around 1300 h, coinciding with F10.7 index intensities of approximately 60–80 sfu. In contrast, during the High Solar Activity (HSA) period, diurnal VTEC peak values of around 50–80 TECU are observed around 1400 h, with F10.7 index intensities around 150–180 sfu.

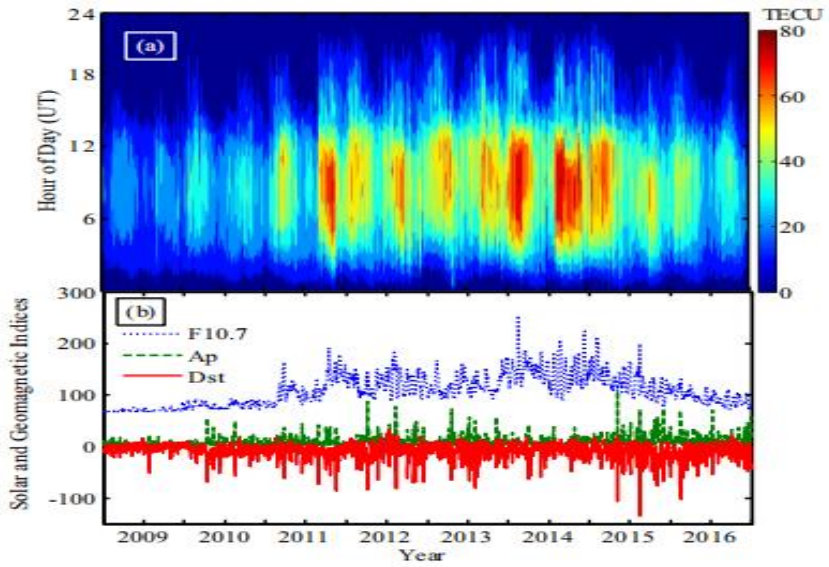

Fig. 2 shows the time series fluctuation of the solar F10.7 index (blue), Ap index (green), and Dst index (red) for the years 2009 to 2016 generated from GPS data. (The reader is directed to the web version of this page for interpretation of the references to colour in this gure legend.)

ISSN PRINT 2319 1775 Online 2320 7876

Research paper UGC CARE Listed (Group -I) Journal Volume 10, Spl Iss 2, 2021

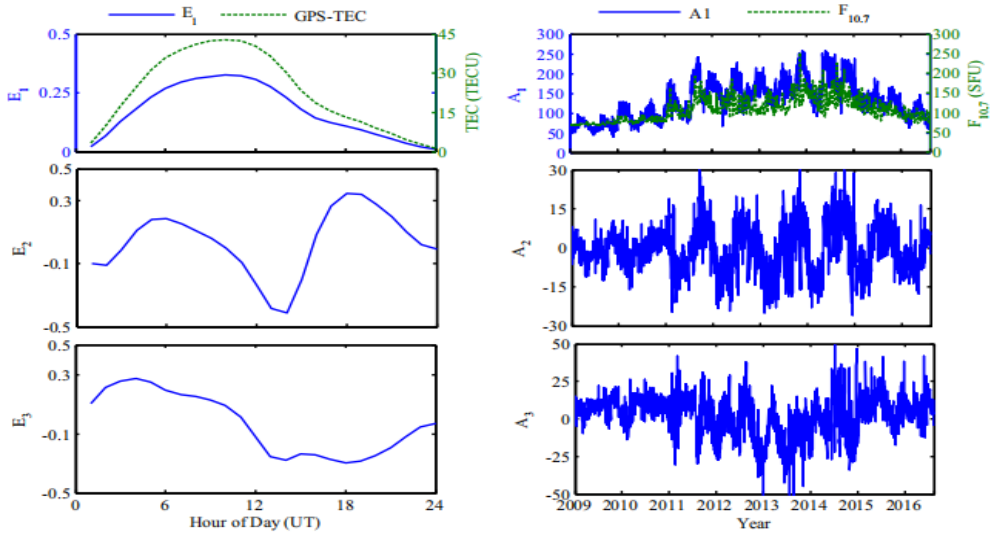

The first three EOF base functions (E) and their corresponding coeficients (A) for the TEC fluctuation over Bangalore station are shown in Fig. 3.

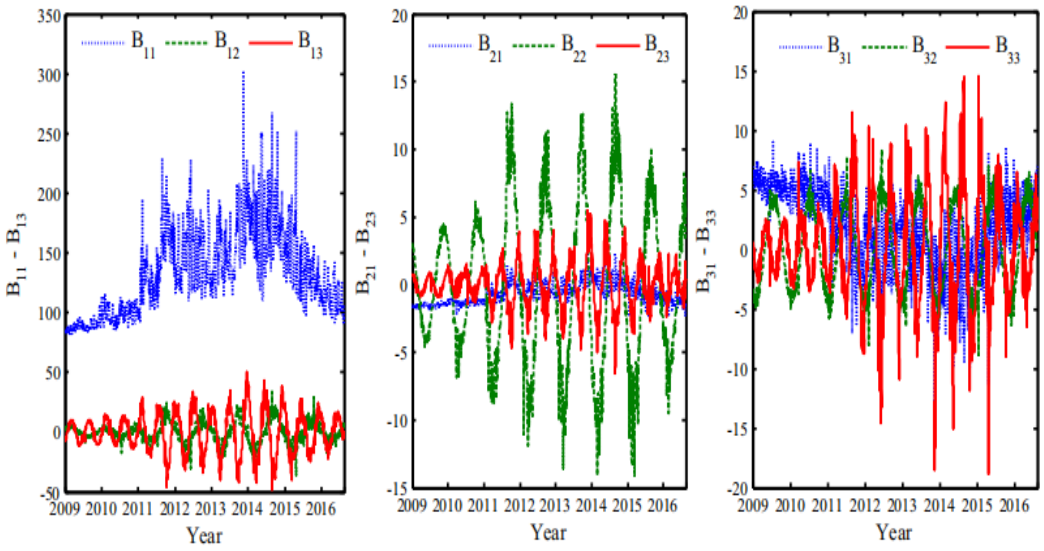

Figure 4 shows the temporal fluctuations of the EOF coecients with various components at Bangalore station.

The rise of the F-region dynamo electric field under the post-sunset deterioration of the E layer conductivity is the primary cause of the PRE occurrence (Abdu, 2005; Fejer, 2011). However, the results of A2 and A3's coecients show that there are annual and semi-annual changes, respectively, with A2's amplitude being comparatively bigger than A3's. Based on the 104 stations in the global ionosonde network, Yu et al. (2004) showed that a similar scenario is also

ISSN PRINT 2319 1775 Online 2320 7876

Research paper **© 2012 IJFANS. All Rights Reserved, UGC CARE Listed (Group -I) Journal Volume 10, Spl Iss 2, 2021**

being seen in the variation of NmF2.The model developed in the study is likely to be valid for other solar cycles because it incorporates averaged daily solar fluxes (F10.7) and geomagnetic activity (Dst and Ap) indices as input parameters for Fourier series analysis. This allows the model to reflect the influence of solar and geomagnetic activities on TEC variations. The first three EOF mode-associated coefficients (A1, A2, and A3) capture the solar-cycle, semi-annual, and annual variations, which are further modulated with solar (F10.7) and geomagnetic (Ap and Dst) indices as shown in Equation (6) of the study (A et al., 2012). This approach ensures that the model is capable of representing the TEC variations for different solar cycles.

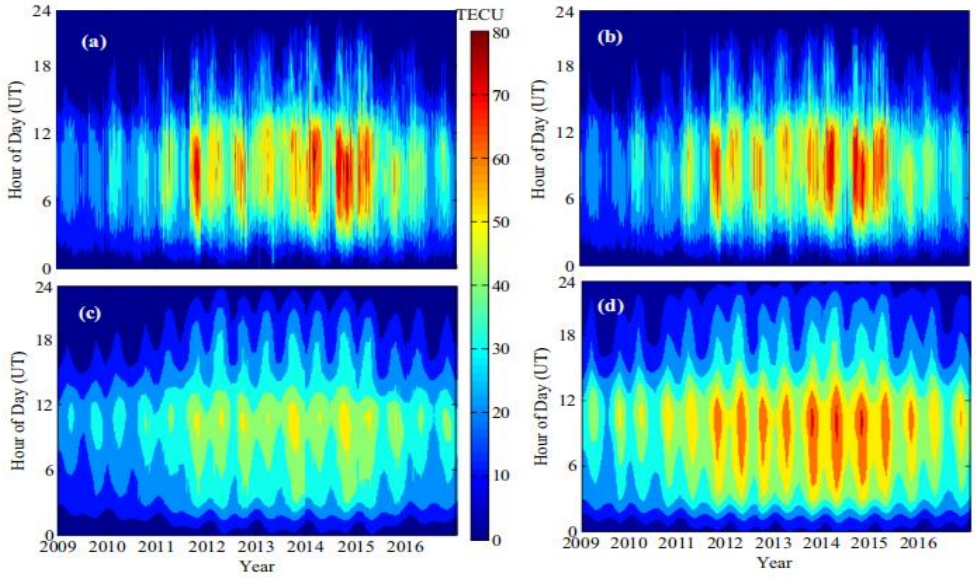

Fig. 5. The time series of the 24th solar cycle's (2009–2016) measured TEC, EOF model, IRI2016 model value, and SPIM model value.

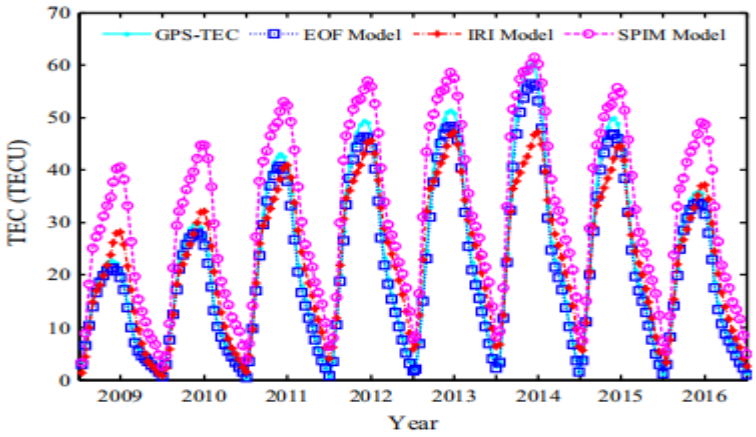

ISSN PRINT 2319 1775 Online 2320 7876

Research paper UGC CARE Listed (Group -I) Journal Volume 10, Spl Iss 2, 2021

Fig. 6. Shows the yearly mean TEC values of observed TEC, EOF model, IRI2016 model and SPIM model over Bangalore during 24th solar cycle(2009–2016).

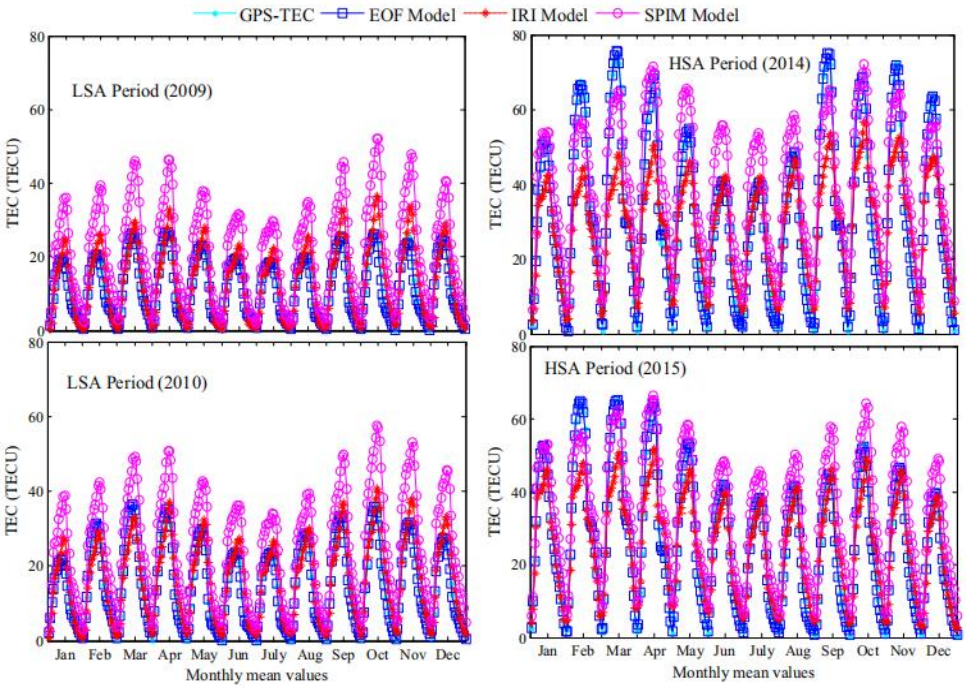

Fig. 7. Shows the monthly mean TEC values of observed GPS-TEC, EOF model, IRI2016 model and SPIM model during LSA periods (2009–2010) and HSA periods (2014–2015).

To validate the accuracy of the EOF model, the yearly mean TEC values obtained from observations are compared with the model-predicted TEC values. The comparison in Fig. 6 shows that the yearly mean trends in observed TEC and EOF model TEC are quite similar to each other. On the other hand, the IRI2016 model tends to overestimate the observed TEC at noon and during sunset hours (by around 2-8 TECU) during the Low Solar Activity (LSA) period and underestimate it (by around 3-10 TECU) during the High Solar Activity (HSA) period. Similarly, the SPIM model tends to overestimate TEC during most of the period (2009-2016) except for the HSA period in 2014, with higher values around noon and sunset hours (around 5-15 TECU). The Root Mean Square Deviation (RMSD) and correlation coefficients between the model TEC values and observed GPS-TEC values for the years 2009-2016 are listed in Table 2. These results indicate that the EOF model performs well in capturing the TEC variations compared to the other standard ionospheric models.

ISSN PRINT 2319 1775 Online 2320 7876

Research paper UGC CARE Listed (Group -I) Journal Volume 10, Spl Iss 2, 2021

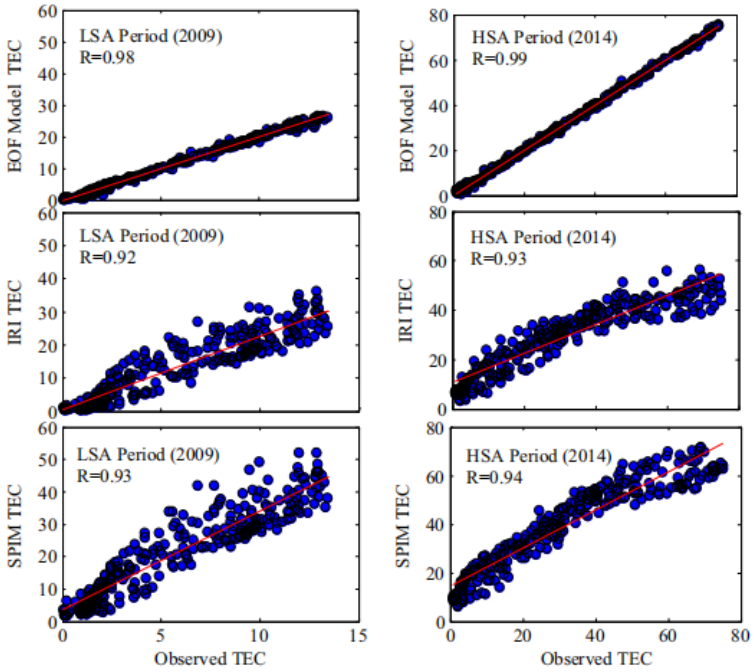

Fig. 8. Scatter plots of EOF, IRI2016 and SPIM model values versus observed GPS-TEC values over Bangalore station.

The observed GPSTEC, EOF model, IRI2016 model, and SPIM model values for the LSA periods (2009–2010) and the HSA periods (2014–2015) are compared in Fig. 7. The graph clearly demonstrates that GPS-TEC magnitude is generally larger during equinoctial months and lower during solstitial months. This confirms the GPS-TEC anomaly over the low latitude, which occurs semi-annually. Rishbeth (2000) showed the semiannual anomaly in the F region ionosphere across middle to low latitude in relation to this. According to Zhao et al. (2008), this phenomenon was explained by the fact that meridional winds have somewhat smaller amplitudes during equinoxes (than solstices), which results in less mixing with nitrogen-rich air and a greater O/N2 ratio. The "thermospheric-spoon" process is the creation of increased densities during equinoxes to result in semiannual anomaly (Fuller-Rowell, 1998).

(Fig. 8). IRI2016 and SPIM models have lower correlation coefficients than the EOF model, which has a correlation coefficient between its values and the observed GPSTEC values of 0.98 and 0.99 for the LSA and HSA periods. According to earlier research on the IRI model, there are significant differences between the model's predictions and the actual GPS-TEC data over the LSA period (Bilitza and Williamson, 2000; Bilitza et al., 2006). Therefore, it is confirmed that the EOF model, by reflecting the temporal distribution characteristics, can represent the original data pretty effectively.

ISSN PRINT 2319 1775 Online 2320 7876

Research paper UGC CARE Listed (Group -I) Journal Volume 10, Spl Iss 2, 2021

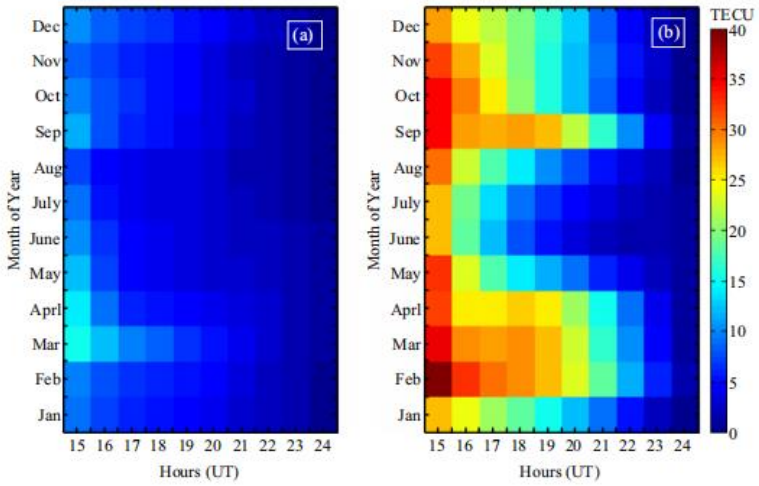

Fig. 10. Diurnal and seasonal variations of the nighttime VTEC over Bangalore for (a) LSA year 2009, (b) HSA year 2014.

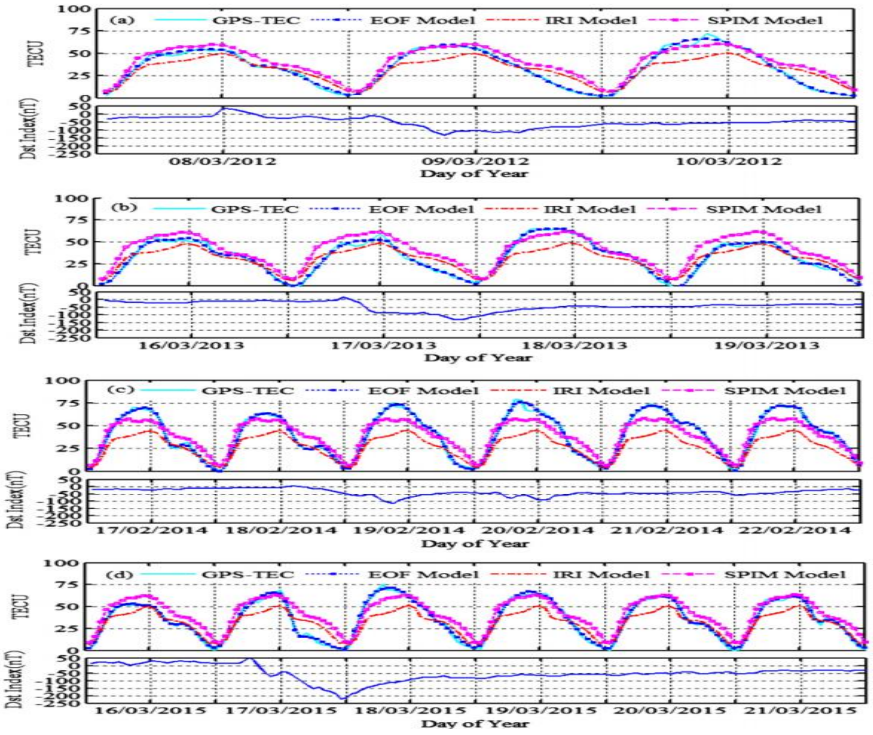

Figure 11 shows a comparison of the GPS-TEC, GS, IRI2016, and SPIM models during the storm occurrences of (a) March 9, 2012, (b) March 17, 2013, (c) February 19, 2014, and (d) March 17, 2015.

Conclusion

ISSN PRINT 2319 1775 Online 2320 7876

Research paper **© 2012 IJFANS. All Rights Reserved, UGC CARE Listed (Group -I) Journal Volume 10, Spl Iss 2, 2021**

The Fourier Series Analysis (FSA) was used to characterize the solar-cycle, annual, and semi-annual dependencies by modulating the first three EOF coefficients with solar (F10.7) and geomagnetic (Ap and Dst) indices. The EOF coefficients were found to be associated with solar and geomagnetic activity, with solar activity being the dominant factor controlling TEC variability.

Comparative analysis between the observed GPS-TEC data, EOF model, and standard global models (IRI2016 and SPIM) revealed that IRI2016 overestimated TEC during low solar activity and underestimated it during high solar activity, while SPIM overestimated TEC for most of the period except the peak solar activity year 2014. In contrast, the EOF model showed better agreement with observed TEC data and provided more accurate predictions of ionospheric variations compared to IRI2016 and SPIM models.

The EOF model proved to be effective in predicting TEC enhancements and depletions during geomagnetic storm conditions. It successfully described diurnal, seasonal, and annual ionospheric variations in GPS-TEC under various solar and geomagnetic conditions.

References

1. A, E., Zhang, D.H., Xiao, Z., Hao, Y.Q., Ridley, A.J., Moldwin, M., 2011. Modeling ionospheric for F2 by using empirical orthogonal function analysis. Ann. Geophys. 29 (8), 1501–1515.
2. A, E., Zhang, D., Ridley, A.J., Xiao, Z., Hao, Y., 2012. A global model: Empirical orthogonal function analysis of total electron content 1999–2009 data. J. Geophys. Res.: Space Phys. 117, A03328.
3. Abdu, M., 2005. Equatorial ionosphere–thermosphere system: electrodynamics and irregularities. Adv. Space Res. 35 (5), 771–787.Araujo-Pradere, E., Fuller-Rowell, T., Codrescu, M., Bilitza, D., 2005.Characteristics of the ionospheric variability as a function of season, latitude, local time, and geomagnetic activity. Radio Sci. 40 (5), RS 5009.
4. Bagiya, M.S., Joshi, H., Iyer, K., Aggarwal, M., Ravindran, S., Pathan, B., 2009. TEC variations during low solar activity period (2005–2007) near the

ISSN PRINT 2319 1775 Online 2320 7876

Research paper UGC CARE Listed (Group -I) Journal Volume 10, Spl Iss 2, 2021

equatorial ionospheric anomaly crest region in India. Ann. Geophys. 27 (3), 1047–1057.

5. Bilitza, D., Reinisch, B.W., 2008. International reference ionosphere 2007: improvements and new parameters. Adv. Space Res. 42 (4), 599–609. Bilitza, D., Williamson, R., 2000. Towards a better representation of the IRI topside based on ISIS and Alouette data. Adv. Space Res. 25 (1),149–152.
6. Bilitza, D., Brown, S.A., Wang, M.Y., Souza, J.R., Roddy, P.A., 2012. Measurements and IRI model predictions during the recent solar minimum. J. Atmos. Solar-Terres. Phys. 86, 99–106.
7. Bilitza, D., Altadill, D., Zhang, Y., et al., 2014. The international reference ionosphere 2012–a model of international collaboration. J. Space Weather Space Clim. 4 (A07), 1–12.
8. Chen, Z., Zhang, S.R., Coster, A.J., Fang, G., 2015. EOF analysis and modeling of GPS TEC climatology over North America. J. Geophys. Res.: Space Phys. 120 (4), 3118–3129.
9. Dabas, R., Das, R., Vohra, V., Devasia, C., 2006. Space weather impact on the equatorial and low latitude F-region ionosphere over India. Ann. Geophys. 24 (1), 97–105.
10. Dabbakuti, J.K., Venkata Ratnam, D., 2016. Characterization of iono-spheric variability in TEC using EOF and wavelets over low-latitude GNSS stations. Adv. Space Res. 57 (12), 2427–2443.
11. Dabbakuti, J.K., Venkata Ratnam, D., Kanchumarthi, S.R., 2016. Analysis of local ionospheric variability based on SVD and MDS at low-latitude GNSS stations. Earth Planets Space 68 (1), 1–11.
12. Dashora, N., Suresh, S., 2015. Characteristics of low-latitude TEC during solar cycles 23 and 24 using global ionospheric maps (GIMs) over Indian sector. J. Geophys. Res.: Space Phys. 120 (6), 5176–5193.
13. Raju, K., Pilli, S. K., Kumar, G. S. S., Saikumar, K., & Jagan, B. O. L. (2019). Implementation of natural random forest machine learning methods on multi spectral image compression. Journal of Critical Reviews, 6(5), 265-273.
14. Saba, S. S., Sreelakshmi, D., Kumar, P. S., Kumar, K. S., & Saba, S. R. (2020). Logistic regression machine learning algorithm on MRI brain image for fast

ISSN PRINT 2319 1775 Online 2320 7876

Research paper UGC CARE Listed (Group -I) Journal Volume 10, Spl Iss 2, 2021

and accurate diagnosis. International Journal of Scientific and Technology Research, 9(3), 7076-7081.